Secondary Coordinated Control of Islanded Microgrids Based on Consensus Algorithms

Wu, Dan; Dragicevic, Tomislav; Vasquez, Juan Carlos; Guerrero, Josep M.; Guan, Yajuan

Published in:
Proceedings of the 2014 IEEE Energy Conversion Congress and Exposition (ECCE)

DOI (link to publication from Publisher):
10.1109/ECCE.2014.6953986

Publication date:
2014

Document Version
Early version, also known as pre-print

Secondary Coordinated Control of Islanded Microgrids Based on Consensus Algorithms

Dan Wu, Tomislav Dragicevic, Juan C. Vasquez, Josep M. Guerrero, Yajuan Guan
Microgrids Research Programme www.microgrids.et.aau.dk
Institute of Energy Technology, Aalborg University, Denmark
{dwu , tdr , juq , joz, ygu}@et.aau.dk

***Abstract*— This paper proposes a decentralized secondary control for islanded microgrids based on consensus algorithms. In a microgrid, the secondary control is implemented in order to eliminate the frequency changes caused by the primary control when coordinating renewable energy sources and energy storage systems. Nevertheless, the conventional decentralized secondary control, although does not need to be implemented in a microgrid central controller (MGCC), it has the limitation that all decentralized controllers must be mutually synchronized. In a clear cut contrast, the proposed secondary control requires only a more simplified communication protocol and a sparse communication network. Moreover, the proposed approach based on dynamic consensus algorithms is able to achieve the coordinated secondary performance even when all units are initially out-of-synchronism. The control algorithm implemented in an islanded microgrid system is tested in different scenarios by means of hardware-in-the-loop results.**

***Index Terms* – Secondary control, frequency control, islanded microgrids, consensus algorithms**

I. INTRODUCTION

Taking the idea from large power systems, frequency control strategies are usually utilized in microgrids to achieve power management among distributed renewable energy sources (RES), energy storage systems (ESS) and loads. In order to enhance reliability and to increase flexibility of coordination performance, many control structures have been investigated, including droop controllers, virtual inertias, and bus signaling, among others [1]-[4]. The aforementioned techniques use frequency deviations to coordinate the controllers with only local measurements.

In [1], centralized and decentralized control systems are described and compared for the power management in microgrids. The centralized control system can be realized with a simple hierarchical control implementation, but the coordination performance may be deteriorated by a single point of communication link failure in the microgrid central controller (MGCC). In the case of a decentralized control structure, the coordination strategies are imposed directly by local controllers. However, advanced communication algorithm to calculate consensus data needs to be developed; otherwise the communication link may hold too much burden to transmit information among distributed units.

Recently, a primary and secondary coordinated control structure between ESS and RES in islanded microgrid has been proposed by the authors in [5]. In this work, the different functions are clearly defined in primary and secondary control levels. The primary coordinated control aims at power regulation of all units based on different state of charge (SoC) scenarios of ESS. Coordination performance can be achieved in a fully decentralized way even without communication links. Meanwhile, secondary coordinated control is implemented to obtain frequency restoration by using communication links. In that sense, both centralized and decentralized control structures can be adopted for the secondary control, as shown in Fig. 1. However, in both cases the system stability and coordinated performance rely on the synchronization of frequency restoration between RES and ESS units throughout communication link. Especially for decentralized secondary control, how to overcome the limitation of synchronization among distributed controllers and at the same time, simplify the communication algorithms for data transmitting needs to be investigated.

The implementation of consensus algorithms for distributed systems has drawn a lot of attention in recent years. Instead of transmitting the data stored in one unit to all units in order to achieve coordination, this method develops an information exchange rule between one unit and all its neighbors to reach the data averaging [6-8], thus making the communication algorithm simpler, practical, and more robust to communication link failures. In [9], dynamic consensus algorithm is proposed and analyzed for dynamic systems where sensing data changes with the time. A detailed analysis of determining weights of nodes along communication links to increase the converging speed is

978-1-4799-5776-7/14/$31.00 ©2014 IEEE

illustrated in [10]. Despite of lots of these discussions of consensus algorithm in computer science area, the application of this algorithm and its advanced forms can also be seen in AC and DC microgrids [13, 14]. In these researches, the droop control and power line communication technique are employed for primary level to realize fully

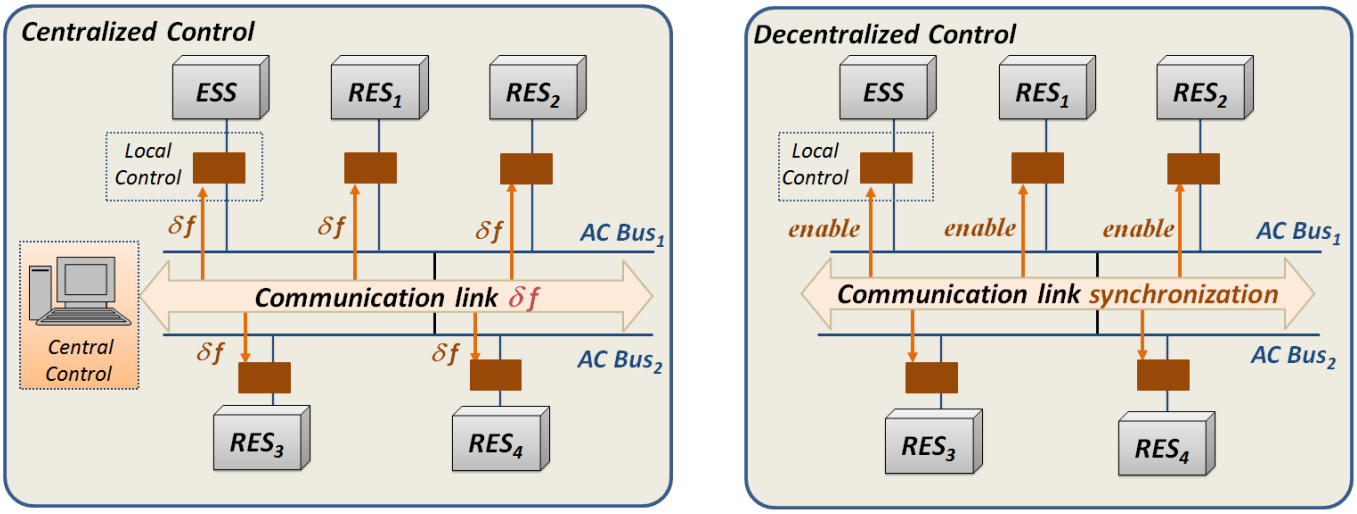

(a) (b)

Figure 1. Centralized and decentralized control structure of microgrids.

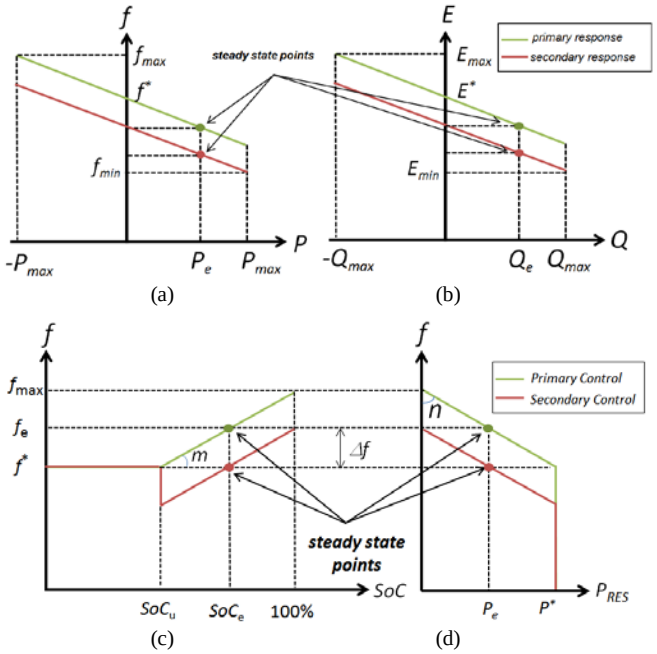

(a) (b) (c) (d)

Figure 2. Primary and secondary control performance: droop control of frequency (a) and voltage amplitude(b), coordinated control of ESS and

decentralized control objective [15, 16]. While secondary control in hierarchical microgrids which is considered as a general form is used to eliminate bus variable deviations (bus frequency and voltage).

In this paper, a consensus algorithm for the decentralized secondary coordinated control is implemented as an extension of our previous work [4]. Firstly, the hierarchical structure based on ESS and RES coordinated control is presented. The dynamic consensus method is utilized in secondary level to avoid the out-of-synchronization distributed units. In this way, the hierarchical control of ESS and RES units can be decentralized not only in primary level but throughout hierarchical level, which adopts only a sparse communication network spanned across microgrid. Additionally, the weight calculation procedure for optimal converging speed is also presented, so that the overall system can find out converged variables in a fast way. Finally, real-time simulation results based on an islanded microgrid are presented to verify the effectiveness of the proposed control.

II. Primary and Secondary Coordinated Control

In islanded microgrids, the output power from ESS and RES units should be controlled in a coordinated way concerning SoC condition so that to keep balance between power generation and consumption, at the same time prevent ESS from over charge scenario. This coordinated objective is fulfilled based on two-level hierarchical control structure: primary level with regards to power electronics control and secondary level for bus variable regulation. In this section, the hierarchical control structure based on coordinated control is illustrated and compared with traditional hierarchical control taking into account droop control strategy.

A. Primary Control Level

Fig. 2(a) and Fig. 2(b) show the hierarchical control (tertiary control of energy management system is not considered here) of microgrid based on droop control. In order to share active and reactive power among voltage

control mode converters, each unit regulates output frequency and voltage amplitude based on its own output power. As a result, steady state bus variable deviation is generated as the figures show.

In a similar way, Fig. 2(c) and Fig. 2(d) show the cooperative control performance for ESS and RES units based on this two level control structure, where ESS unit operates as master unit controlling bus frequency with SoC condition (see Fig. 2(c)), and RES units work as slave units regulating output power according to bus frequency condition (see Fig. 2(d)). Therefore, the bus frequency is presented as an information link carrying ESS condition to inform RES units for power regulation. In this paper, only frequency bus signaling is discussed as an example since the energy stored in ESS which exchange with RES and provide to loads is related directly with active power while reflected by SoC.

According to different SoC conditions, bus frequency is controlled at different values. When ESS is not approaching to be fully charged, bus frequency is controlled at nominal value while power generated by RES units is regulated at reference P^*. When SoC is high and beyond up-threshold SoC_u, bus frequency is boosted as a function of SoC. In this range, power generated from RES is decreased as a function of bus frequency. In this range, similar with conventional droop control [11], the bus frequency is deviated from nominal value as shown in Fig. 2(c) and Fig. 2(d). The coordinated control strategies for ESS and RES units respectively are expressed as

$$\begin{cases} f = f^* & SoC \le SoC_u \\ f = f^* + m \cdot (SoC - SoC_u) & SoC_u < SoC < 100\% \end{cases} \quad (1)$$

$$\begin{cases} P_{RES} = P^* & f \le f^* \\ P_{RES} = P^* - n \cdot (f - f^*) & f > f^* \end{cases} \quad (2)$$

where f^* is nominal frequency value and SoC_u is up-threshold of SoC, P_{RES} is power generated from RES units, and P^* is its constant power reference (usually refers to maximum power point based on prime source condition), m and n are the frequency boosting and power dropping slopes for ESS and RES respectively. Since both start and final points of frequency boosting and power dropping lines for ESS and RES are determined, m and n can be calculated as

$$m = \frac{f_{\max} - f^*}{100\% - SoC_u} \quad (3)$$

$$n = \frac{P^*}{f_{\max} - f^*} \quad (4)$$

where $f_{\max}$ is maximum frequency value.

It can be seen from Fig. 2 that with only primary coordinated control, steady state bus frequency deviation Δf will be produced as P_{RES} decreases to steady state point P_e, Although maximum frequency deviation of Δf can be designed within an allowable range according to (1), it can also be eliminated by secondary control when tight bus frequency regulation is required.

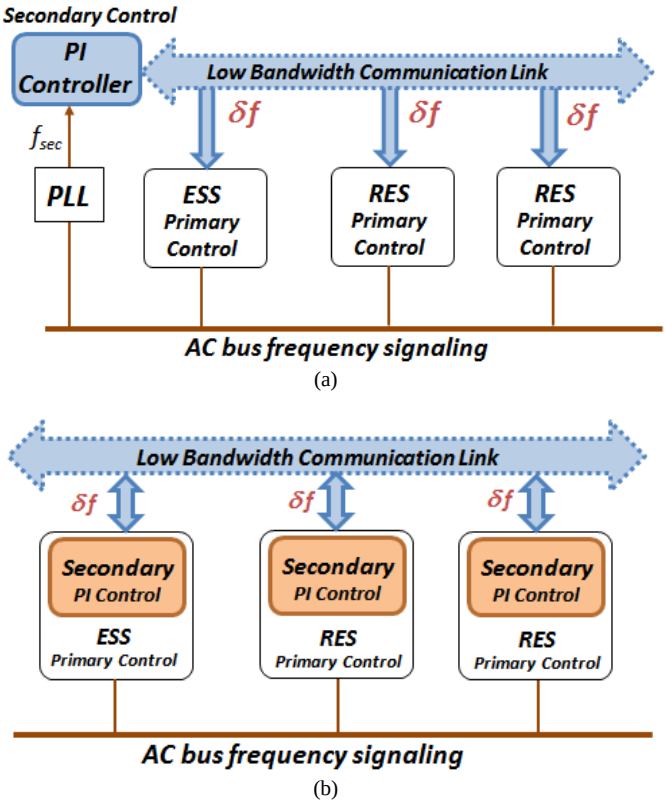

Figure 3. Secondary control configuration in centralized (a) and decentralized configuration.

B. Secondary Control Level

In droop controlled hierarchical structure, secondary controller is utilized to adjust frequency and voltage amplitude set-points, while local primary controller remains the same control algorithm and receives the updated set-points, as shown in Fig. 2(a) and Fig. 2(b). Similarly in coordinated control strategy, when SoC of ESS is operating in normal range, the secondary control is not enabled and coordinated performance remains the same as primary control. When $SoC > SoC_u$, both response of the ESS and RES units shift downward by the restoration term δf sent from secondary controller. This restoration term δf is regulated by secondary proportional integral (PI) controller which is expressed as

$$\delta f = G_s(s) \cdot (f^* - f_{\sec}) = \left(k_{p\sec} + \frac{k_{i\sec}}{s} \right) \cdot (f^* - f_{\sec}) \quad (5)$$

where $G_s(s)$ is secondary controller with $k_{p\sec}$ and $k_{i\sec}$ as proportional and integral terms. $f_{\sec}$ is the measured bus

frequency by secondary controller. Hence, with the secondary restoration term δf, the ESS and RES coordinated control in (1) and (2) can be rewritten as

$$f = f^* + \delta f + m \cdot (SoC - SoC_u) \quad SoC_u < SoC < 100\% \quad (6)$$

$$P_{RES} = P^* - n \cdot (f - f^* - \delta f) \quad f > f^* + \delta f \quad (7)$$

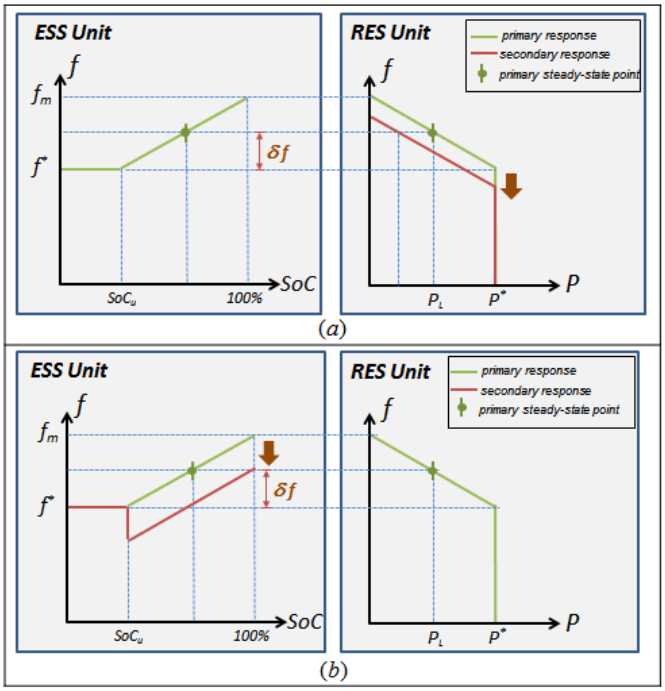

Figure 4. Different scenarios of secondary control: lose secondary control in ESS (a) and RES (b) and both (c).

Fig. 3 shows centralized and decentralized secondary control algorithm. Compare Fig. 3(b) with Fig. 3(a), the decentralized control structure can avoid single point communication failure in the MGCC. However, the conventional distributed secondary control strategy needs to be synchronized to calculate a consensus δf [12]. Fig. 4(a) and Fig. 4(b) show the scenarios when ESS and RES secondary controllers are out-of-synchronization. When the decentralized secondary control of RES starts up earlier than ESS (Fig. 4(a)), it causes that bus frequency deviation is not eliminated temporally, while the coordination curve of RES shift downward due to the secondary control effect. Then, the power generation is smaller than power of loads, resulting in a decrease of SoC. When SoC decreases below the up-threshold, power generation is larger than power of loads and SoC increases. In the most serious case that secondary control of ESS is not started yet when power generated from RES decreases to power of loads, the system will oscillate around the upper SoC threshold. In case of secondary control of ESS starts up earlier than RES (see Fig. 4(b)), the bus frequency deviation can be suppressed by the secondary control of ESS. However, the RES will generate power larger than power of loads continuously since they have not received the signal of secondary control that shift down the curve. In a critical case in which the bus frequency is restored to the nominal value, while RES units are not enabled, the overcharge situation may happen and the system may loss the coordination performance.

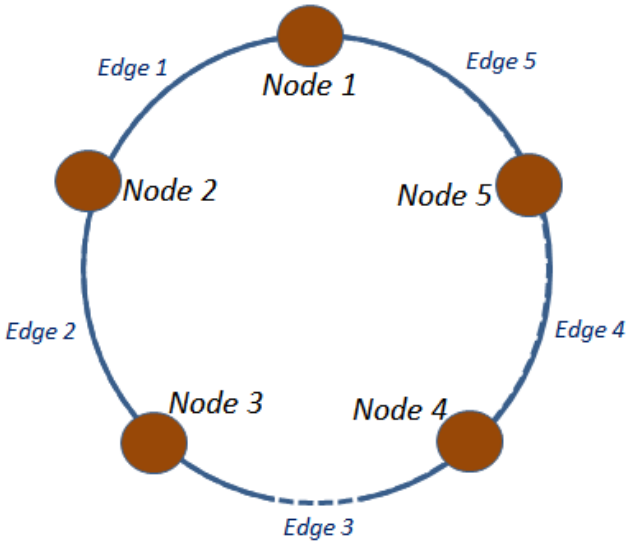

Figure 5. Example of network with consensus algorithm (n=5).

III. Consensus Algorithm for Decentralized Systems

For decentralized secondary controller, each unit needs to exchange data with other units in order to obtain a consensus on δf value. When the number of distributed unit increases, more and more data needs to be communicated, which may result in communication jam. Therefore there is a need for the decentralized structure to employ a clear and simple algorithm to reduce the burden of communicating data stored in each unit. Instead of exchanging data with all other units, a distributed consensus algorithm is proposed to connect all units. Fig. 5 shows a connected graph of 5 nodes. The consensus algorithm only requires that each node in the system communicates with its neighbors, and then the overall connected system is able to reach an agreement of the data stored in units. Here in this example all the units are connected in a ring to compute the average value. In distributed consensus algorithm there is no need to connect each unit to other units directly. Only if each unit has a channel connected to other units the system can finally reach an agreement. Therefore this topology of secondary control is more suitable for system that components are distributed located. Notice in Fig. 5 that even with any one of the communication link disconnected, the system still can reach an average value since every node has an auxiliary channel to other units.

In a general case, a connected distributed system with $Sys=(N,E)$ can be presented as multiple nodes $N=\{1..,n\}$ and

a set of edge *E*. Here each edge *E* is defined as $\{i, j\}\in E$, where *i* and *j* present the two different nodes connected by edge. For node *i*, its set of neighbors is defined as $N_i=\{j|\{i,j\}\in E\}$. The distributed consensus algorithm needs iteration steps to calculate an agreement value, the data stored is denoted as $x_i(k)$ with *k* being the iteration step. Then the iterative form of basic consensus algorithm can be described as

$$x_i(k+1)=x_i(k)+\sum_{j\in N_i}\alpha_{ij}(x_j(k)-x_i(k)) \tag{8}$$

where α_{ij} is the weight on x_j at node *i*. In this case, each node collects information from all its neighbors and multiplies by a weight to update the stored value, then sends out its own information. Based on this iteration procedure all nodes can achieve a final average value with a simple communication configuration. In order to obtain good consensus performance, two aspects should be taken into consideration: i) determine proper weight for each node for a fast iteration process to consensus, ii) develop improved algorithm based on (8), so that dynamic data stored in each node can be modified.

In order to obtain fast iterate weights of each node, the incidence matrix $\boldsymbol{A}\in\boldsymbol{R}^{N\times E}$ can be developed for distributed system *Sys* as

$$A_{il}=\begin{cases}1 & \text{if edge } l \text{ starts from node } i\\ -1 & \text{if edge } l \text{ ends at node } i\\ 0 & \text{if node } i \text{ and edge } l \text{ are not connected}\end{cases} \tag{9}$$

where A_{il} is component of $\boldsymbol{A}$ representing relationship of node $i\in N$ and edge $l\in E$. The incidence matrix indicating system configuration of how components are connected together. With incidence matrix, the Laplacian matrix of system can also be written as $\boldsymbol{L}=\boldsymbol{A}\boldsymbol{A}^{\mathrm{T}}$. Take Fig. 5 for example, considering all nodes are connected in a counterclockwise way, the incidence matrix and corresponding Laplacian matrix can be expressed respectively as

$$A=\begin{bmatrix}1&0&0&0&-1\\-1&1&0&0&0\\0&-1&1&0&0\\0&0&-1&1&0\\0&0&0&-1&1\end{bmatrix} \tag{10}$$

$$L=\begin{bmatrix}2&-1&0&0&-1\\-1&2&-1&0&0\\0&-1&2&-1&0\\0&0&-1&2&-1\\-1&0&0&-1&2\end{bmatrix} \tag{11}$$

Here we adopt a constant weight α implementing on all units for simplicity. Then the fast distributed consensus problem can be formulated as [10]

$$\text{minimize}\quad \left\|I-\alpha\cdot L\right\|_2 \tag{12}$$

where $\|\cdot\|_2$ is spectrum norm of I-α·L. Then the optimal constant weight for fast iteration can be given as

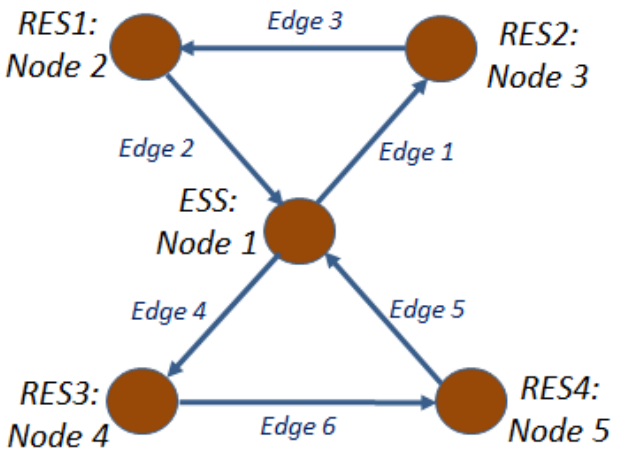

Figure 6. Consensus algorithm based on islanded microgrid in Fig. 1(b).

$$\alpha^*=\frac{2}{\lambda_1(L)+\lambda_{N-1}(L)} \tag{13}$$

where λ_1 and λ_{N-1} represent the largest and second least eigenvalue of $\boldsymbol{L}$. With optimal weight (8) can be rewritten as

$$x_i(k+1)=x_i(k)+\alpha^*\sum_{j\in N_i}(x_j(k)-x_i(k)) \tag{14}$$

In the case of distributed secondary control, all secondary controllers may not start up at the same time. Therefore consensus algorithm needs to be adapted to scenarios that inputs dynamically changing. Based on (14), a dynamic consensus algorithm can be employed as [9]

$$x_i(k+1)=z_i(0)+\alpha^*\sum_{j\in N_i}\delta_{ij}(k+1) \tag{15}$$

$$\delta_{ij}(k+1)=\delta_{ij}(k)+x_j(k)-x_i(k) \tag{16}$$

where δ_{ij} (*k*) is a cumulative difference between two neighbors, and $z_i(0)$ is initial value. In this case, when different nodes in distributed system are not enabled in a synchronization way, which means δf is updated in real time, the overall distributed system still can converge to average value since dynamic algorithm is directly dependent on inputs $z_i(0)$.

IV. Consensus Algorithm Implementation

An islanded microgrid model with decentralized secondary control structure is developed based on Fig. 1(b), consisting of one ESS unit and four RES units connected to two buses. The communication prototype of decentralized secondary control is shown in Fig. 6, based on dynamic consensus algorithm. Noticed here that this dynamic

consensus algorithm is not constrained to forms of local controller, and can not only be implemented in coordinated control structure but also share the same algorithm with hierarchical control based on droop control strategy.

TABLE I. Coordinated control parameters

Item	Symbol	Value
Maximum frequency threshold	f_1	51Hz
Nominal bus frequency	f^*	50Hz
Nominal bus voltage amplitude	E^*	230V
SoC *upper limit*	SoC_1	95%
Secondary frequency reference	$f_{\sec}$	50Hz
Secondary control proportional term	$k_{p\sec}$	0.005
Secondary control integral term	$k_{i\sec}$	0.5 s^{-1}
Constant weight of consensus algorithm	α^*	1/3
ESS voltage controller	k_{pV}, k_{iV}	0.1, 100s^{-1}
ESS current controller	k_{pI}, k_{iI}	15, 50s^{-1}
RES current controller	k_{pVR}, k_{iVR}	20, 50s^{-1}

The sequence of nodes N is denoted as Node 1 to Node 5 in Fig. 6. And the sequence of edges E is shown as Edge 1 to Edge 6. Since ESS operates as master unit and defines the bus frequency and voltage so that it has more communication exchange with other units to ensure the total system robustness. According to (10) and (11) and definition in (9), the incidence matrix and Laplacian matrixes are developed as

$$A=\begin{bmatrix} 1 & -1 & 0 & 1 & -1 & 0 \\ 0 & 1 & -1 & 0 & 0 & 0 \\ -1 & 0 & 1 & 0 & 0 & 0 \\ 0 & 0 & 0 & -1 & 0 & 1 \\ 0 & 0 & 0 & 0 & 1 & -1 \end{bmatrix} \tag{17}$$

$$L=\begin{bmatrix} 4 & -1 & -1 & -1 & -1 \\ -1 & -2 & -1 & 0 & 0 \\ -1 & -1 & 2 & 0 & 0 \\ -1 & 0 & 0 & 2 & -1 \\ -1 & 0 & 0 & -1 & 2 \end{bmatrix} \tag{18}$$

The largest and second least eigenvalue of $\boldsymbol{L}$ based on (18) can be calculated as $\lambda_1=5$ and $\lambda_{N-1}=1$ respectively, therefore the constant edge weight is deduced as $\alpha^*=1/3$. Then replacing α^* into (15) and (16), the dynamic iteration process for each unit can be obtained. The storage data $x_i(k)$ in each unit represents δf received in each unit.

The primary and secondary control algorithm is shown in Fig. 7, and detailed description of coordinated control implementation is presented in [4]. The distributed secondary control shares a common control structure of ESS and RES units as shown in Fig. 7, where δf_p is output value of secondary PI controller of local unit. And δf_{pN} presents output value of secondary PI controller neighbor units. The control parameters are shown in Table I.

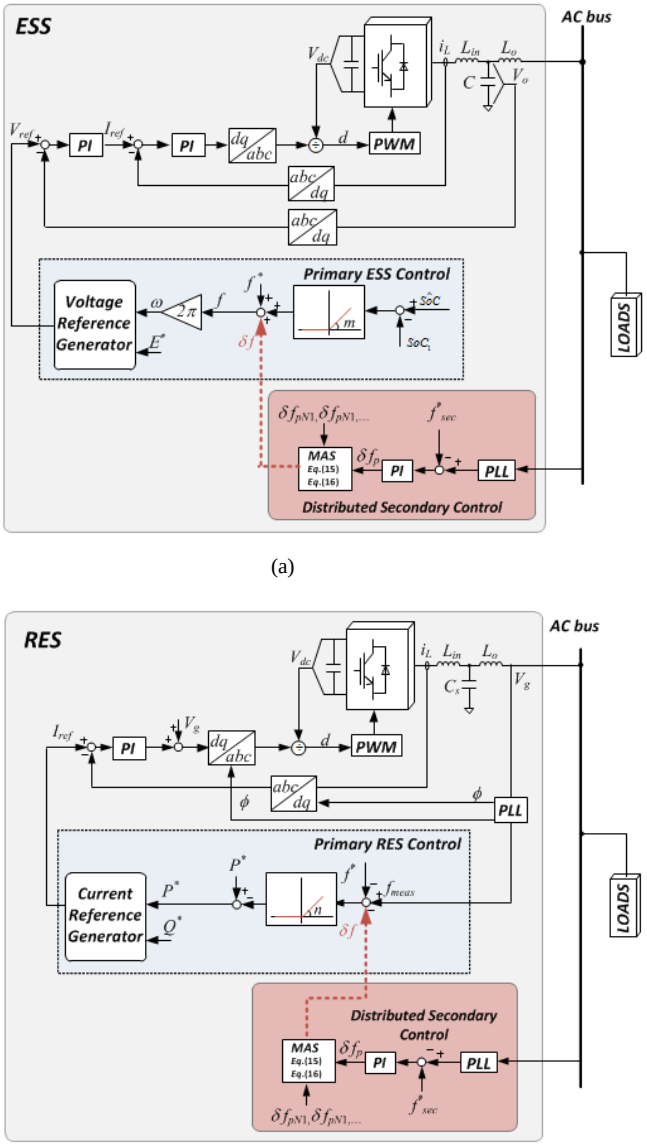

Figure 7. Primry and secondary control algorithm implementation for ESS (a) and RES units (b).

V. Real-time Simulation Results

The proposed coordinated control based on distributed secondary control is tested through dSPACE platform in real time simulation. The simulated system consists one ESS and four RES units, and distributed secondary control is configured in Fig. 6. The controller parameters are described the same in Table I.

Fig. 8 shows the simulation results of coordinated control based on consensus algorithm. In t_1, the SoC of ESS is below up-threshold 95% so that overall system operates in normal range and all RES units produced constant power. When the SoC is above the up-threshold in t_2, the primary coordinated control is performed to decrease all power of RES units to limit charging power of ESS. In steady state of t_2, the power

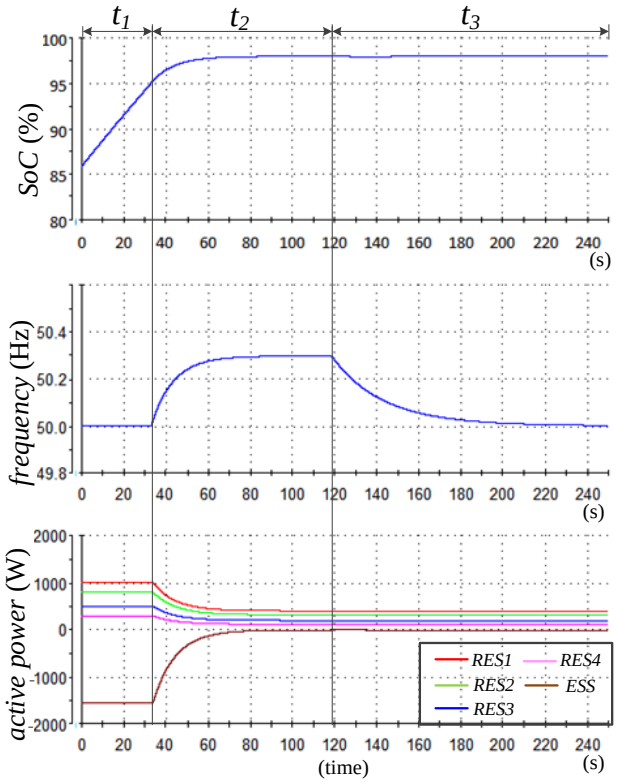

Figure 8. Coordinated performance based on distributed consesus algorithm.

charging to ESS can be limited near to zero. The bus frequency deviation is generated to 50.3Hz due to the distributed primary control. To test the consensus algorithm performance, the simulation studies a severe case that only one secondary controller (*RES1*) is enabled in in t_3, and secondary control of all other four units is not enabled. It can be seen from the result that the bus frequency can be restored to nominal value 50Hz while the coordinated performance of primary control is maintained.

Fig. 9 shows the simulation results when distributed secondary controllers of all units start up at different time. After the bus frequency is boosted by primary control, the distributed secondary control is enabled in a sequence manner. As a result, the output values of PI controller are also calculated as different values at different time range. However, it can be seen that the secondary coordinated control is still effective to restore the bus frequency to nominal frequency in the case out-of synchronization of all secondary controller.

VI. CONCLUSION

A decentralized secondary coordinated control based on consensus algorithm was proposed in this paper. The different scenarios when ESS and RES units are out-of-synchronized for the decentralized secondary control were described and discussed. Then dynamic consensus algorithm is developed and implemented in order to deal with the out-of-synchronization situation. Then in order to achieve good

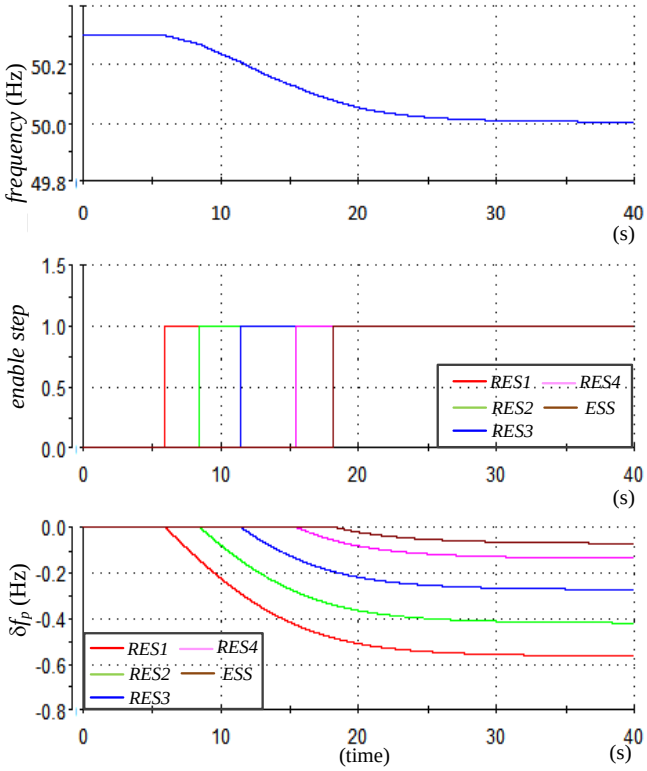

Figure 9. Performance of distributed consesus algorithm based on different start up time.

dynamic response of secondary control in the consensus process, the constant weight for fast iteration was calculated, and advanced form of dynamic consensus algorithm is presented. Finally hardware-in-the-loop results are given so that verified the effectiveness of the proposed controls strategy implementation.

REFERENCES

[1] C. Yuen, A. Oudalov, and A. Timbus, "The Provision of Frequency Control Reserves From Multiple Microgrids," *IEEE Trans. Ind. Electron.*, vol. 58, no. 1, pp. 173–183, Jan. 2011.

[2] Jong-Yul Kim, Jin-Hong Jeon, Seul-Ki Kim, Changhee Cho, June-Ho Park, Hak-Man Kim, and Kee-Young Nam, "Cooperative Control Strategy of Energy Storage System and Microsources for Stabilizing the Microgrid during Islanded Operation," *IEEE Trans. Power Electron.*, vol. 25, no. 12, pp. 3037–3048, Dec. 2010.

[3] D. Wu, J. M. Guerrero, J. C. Vasquez, T. Dragicevic, and F. Tang, "Coordinated power control strategy based on primary-frequency-signaling for islanded microgrids," in *Energy Conversion Congress and Exposition (ECCE), 2013 IEEE*, 2013, pp. 1033–1038.

[4] K. T. Tan, X. Y. Peng, P. L. So, Y. C. Chu, and M. Z. Q. Chen, "Centralized Control for Parallel Operation of Distributed Generation Inverters in Microgrids," *IEEE Trans. Smart Grid*, vol. 3, no. 4, pp. 1977–1987, Dec. 2012.

[5] D. Wu, F. Tang. T. Dragicevic, J. C. Vasquez, and J. M. Guerrero, "Coordinated primary and secondary control with frequency-bus-signaling for distributed generation and storage in islanded microgrids," in *IECON 2013 - 39th Annual Conference of the IEEE Industrial Electronics Society*, 2013, pp. 7140–7145.

[6] R. Olfati-Saber, J. A. Fax, and R. M. Murray, "Consensus and Cooperation in Networked Multi-Agent Systems," *Proc. IEEE*, vol. 95, no. 1, pp. 215–233, Jan. 2007.

[7] R. Olfati-Saber, "Flocking for Multi-Agent Dynamic Systems: Algorithms and Theory," *IEEE Trans. Automat. Contr.*, vol. 51, no. 3, pp. 401–420, Mar. 2006.

[8] R. W. Beard, "Consensus seeking in multiagent systems under dynamically changing interaction topologies," *IEEE Trans. Automat. Contr.*, vol. 50, no. 5, pp. 655–661, May 2005.

[9] D. Spanos, R. Olfati-Saber, and R. Murray, "Dynamic consensus on mobile networks," in IFAC World Congress, 2005.

[10] L. Xiao and S. Boyd, "Fast linear iterations for distributed averaging,"Systems & Control Letters, vol. 53, no. 1, pp. 65 – 78, 2004.

[11] Guerrero, J.M.; Chandorkar, M.; Lee, T.; Loh, P.C., "Advanced Control Architectures for Intelligent **Mic**rogrids—Part I: Decentralized and Hierarchical Control," Industrial Electronics, IEEE Transactions on , vol.60, no.4, pp.1254,1262, April 2013.

[12] Q. Shafiee, J. M. Guerrero, and J. C. Vasquez, "Distributed Secondary Control for Islanded Microgrids—A Novel Approach," *IEEE Trans. Power Electron.*, vol. 29, no. 2, pp. 1018–1031, Feb. 2014.

[13] A. Bidram, A. Davoudi, F. L. Lewis, and J. M. Guerrero, "Distributed Cooperative Secondary Control of Microgrids Using Feedback Linearization," *IEEE Trans. Power Syst.*, vol. 28, no. 3, pp. 3462–3470, Aug. 2013.

[14] V. Nasirian, S. Moayedi, A. Davoudi, and F. Lewis, "Distributed Cooperative Control of DC Microgrids," *IEEE Trans. Power Electron.*, vol. PP, no. 99, pp. 1–1, 2014.

[15] A. Micallef, M. Apap, C. S. Staines, and J. M. Guerrero Zapata, "Secondary control for reactive power sharing and voltage amplitude restoration in droop-controlled islanded microgrids," in *2012 3rd IEEE International Symposium on Power Electronics for Distributed Generation Systems (PEDG)*, 2012, pp. 492–498.

[16] H. Liang, B. Choi, W. Zhuang, X. Shen, A. A. Awad, and A. Abdr, "Multiagent coordination in microgrids via wireless networks," *IEEE Wireless Communications*, vol. 19. pp. 14–22, 2012.